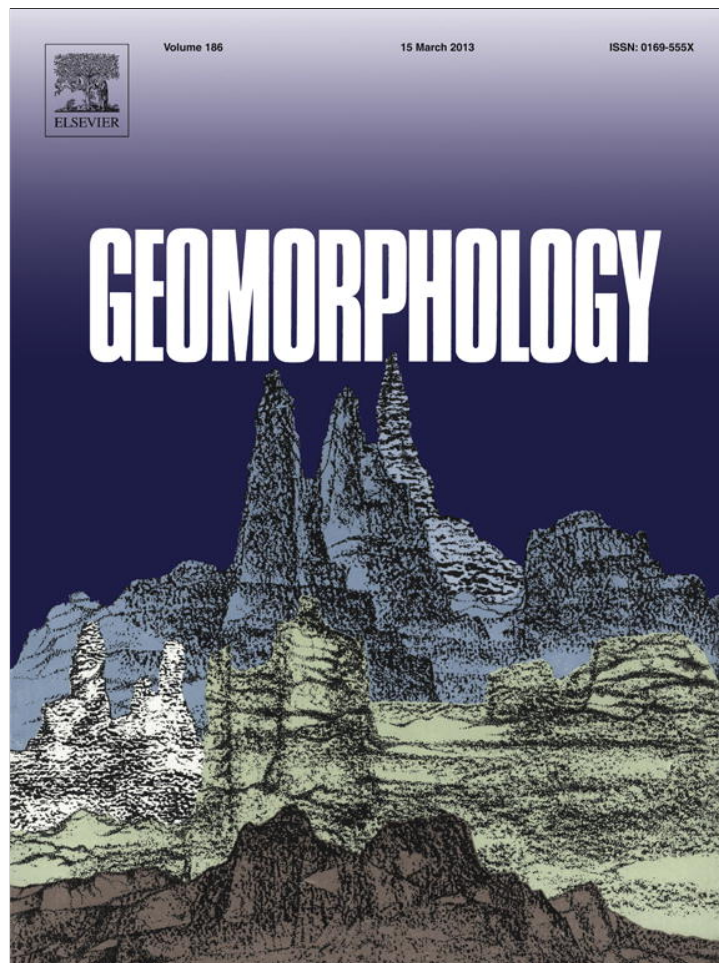


Provided for non-commercial research and education use.
Not for reproduction, distribution or commercial use.

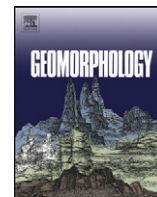


This article appeared in a journal published by Elsevier. The attached copy is furnished to the author for internal non-commercial research and education use, including for instruction at the authors institution and sharing with colleagues.

Other uses, including reproduction and distribution, or selling or licensing copies, or posting to personal, institutional or third party websites are prohibited.

In most cases authors are permitted to post their version of the article (e.g. in Word or Tex form) to their personal website or institutional repository. Authors requiring further information regarding Elsevier's archiving and manuscript policies are encouraged to visit:

<http://www.elsevier.com/copyright>



Analysis of past and future dam formation and failure in the Santa Cruz River (San Juan province, Argentina)

Ivanna M. Penna^{a,b,c,*}, Marc-Henri Derron^a, Michele Volpi^a, Michel Jaboyedoff^a

^a Research Centre for Terrestrial Environment – CRET, University of Lausanne, Geopolis 3156, CH-1015 Lausanne, Switzerland

^b Departamento de Ciencias Geológicas, Facultad de Ciencias Exactas y Naturales, Universidad de Buenos Aires, Ciudad Universitaria, Pabellón II, 1427, Buenos Aires, Argentina

^c Consejo Nacional de Investigaciones Científicas y Técnicas-CONICET, Buenos Aires, Argentina

ARTICLE INFO

Article history:

Received 26 June 2012

Received in revised form 7 December 2012

Accepted 10 December 2012

Available online 22 December 2012

Keywords:

Landslide

DAN3D

Landslide dam failure

Andes

Argentina

ABSTRACT

Around $11.5 \times 10^6 \text{ m}^3$ of rock detached from the eastern slope of the Santa Cruz valley (San Juan province, Argentina) in the first fortnight of January 2005. The rockslide–debris avalanche blocked the course, resulting in the development of a lake with maximum length of around 3.5 km. The increase in the inflow rate from 47,000–74,000 m^3/d between April and October to 304,000 m^3/d between late October and the first fortnight of November, accelerated the growing rate of the lake. On 12 November 2005 the dam failed, releasing $24.6 \times 10^6 \text{ m}^3$ of water. The resulting outburst flood caused damages mainly on infrastructure, and affected the facilities of a hydropower dam which was under construction 250 km downstream from the source area. In this work we describe causes and consequences of the natural dam formation and failure, and we dynamically model the 2005 rockslide–debris avalanche with DAN3D. Additionally, as a volume $\sim 24 \times 10^6 \text{ m}^3$ of rocks still remain unstable in the slope, we use the results of the back analysis to forecast the formation of a future natural dam. We analyzed two potential scenarios: a partial slope failure of $6.5 \times 10^6 \text{ m}^3$ and a worst case where all the unstable volume remaining in the slope fails. The spreading of those potential events shows that a new blockage of the Santa Cruz River is likely to occur. According to their modeled morphometry and the contributing watershed upstream the blockage area, as the one of 2005, the dams would also be unstable. This study shows the importance of back and forward analysis that can be carried out to obtain critical information for land use planning, hazards mitigation, and emergency management.

© 2012 Elsevier B.V. All rights reserved.

1. Introduction

Landslides constitute a major direct hazard in most mountainous regions. Also, catastrophic failure of landslide-dammed lakes causes large magnitude outburst floods that can affect population and critical infrastructure (lifelines, hydropower dams, etc.), even in areas located a thousand kilometers far from the dam (Hewitt, 1982, 1985; Costa and Schuster, 1988; Clague and Evans, 1994; Hewitt, 1998; González Díaz et al., 2001; Dai et al., 2005; Evans et al., 2011). In Argentina, because of its demographic distribution, the direct impact of landslide is lower than in other countries of the Andean Cordillera. However, historical events have shown that many populations in the foreland area are exposed to sudden floods triggered by natural dams breaching in the mountain area. Recently, Hermanns et al. (2011a), based on an inventory of 61 cases of landslide dams, showed that in the eastern side of the central Andes around 11% of the dams failed catastrophically, though the amount could be greater because $\sim 50\%$ of causes of breach

are not known. The largest disaster caused by a dam failure occurred in the northern part of the Neuquén province, where a landslide-dammed lake 22 km long collapsed during the summer of 1914. The sudden release of around 1.55 km^3 of water caused 155 fatalities and affected infrastructures along $\sim 1000 \text{ km}$ from the Main Cordillera to the Atlantic Ocean (González Díaz et al., 2001; Evans et al., 2011). The degree of primary and secondary hazard posed by this kind of events derives from a combination of geomorphologic and environmental conditions. The complete damming of a river depends mainly on the relationship between the morphometry of the valley floor and the volume and dynamics of the rockslide (Costa and Schuster, 1988; Hermanns et al., 2011b). The time that a dam can last until its collapse will depend on water inflow (related to catchment area upstream of the dam and climatic conditions), its morphometry (shape, thickness, and width), and rate of seepage through the dam (Costa and Schuster, 1988; Ermini and Casagli, 2003; Korup, 2004; Hermanns et al., 2011b). A catastrophic dam failure can also be triggered by a rock mass falling into a lake (Hermanns et al., 2004). As all those factors determine the maximum capacity of the water reservoir, they also relate to the magnitude of the outburst flood in case of catastrophic dam breach. Therefore, forecasting the direction of propagation of the landslide and its depositional geometry is essential in assessing hazards related to dam formation and

* Corresponding author at: Departamento de Ciencias Geológicas, Facultad de Ciencias Exactas y Naturales, Universidad de Buenos Aires, Ciudad Universitaria, Pabellón II, 1427, Buenos Aires, Argentina. Tel.: +41 21 692 35 42; fax: +41 21 692 35 35.

E-mail address: ivanna.penna@unil.ch (I.M. Penna).

failure, mitigation, and emergency management. In the last years, back analyses of past events carried out with DAN3D (McDougall and Hungr, 2005) allowed to calibrate the dynamic behavior of landslides, showing their utility to rapidly forecast and with few input data primary hazards (Sosio et al., 2008; Hungr and McDougall, 2009; Hungr, 2011).

In January 2005, a slope collapse built a natural dam in the upper part of the Santa Cruz River tributary of the San Juan River, one of largest rivers in the San Juan province (D'Odorico et al., 2009; Fig. 1). The 12 November 2005 the dam failed catastrophically, producing a flood over 250 km downstream (Perucca and Esper Angillieri, 2009). The aim of this work is to model the dynamics of the rock mass that produced the natural dam in 2005 (back analysis), and to document the changes in the valley morphology (erosion, sedimentation and changes of stream path) caused by the outburst flood. The final goal is, based on the results of the back analysis, to evaluate the likelihood and magnitude of future landslides occurrence as a volume of unstable rock still remains on the slope (forward analysis). The study shows that it is possible to extract critical information about the likelihood of landslide

dam formation in almost inaccessible areas and using publically available data sets.

2. Regional setting

The Santa Cruz range (Fig. 1) is located on the eastern slope of the central Andes, in a sector where the subduction of the Nazca plate is subhorizontal, referred as Pampean flat slab (Baranzagi and Isacks, 1976). Tectonically, this sector of the Andes corresponds to the northern segment of the La Ramada fault and thrust belt, where compressive structures are the result of the Cenozoic tectonic inversion of Triassic normal faults (Ramos et al., 1993; Cristallini, 1996; Alvarez and Ramos, 1999). Although this sector is one of the most seismically active of Argentina, seismicity distribution shows considerably less shallow earthquakes (hypocenter < 100 km deep) than in the trench area (located ~200 km west) or in the Precordillera (120 km east; Pardo et al., 2002).

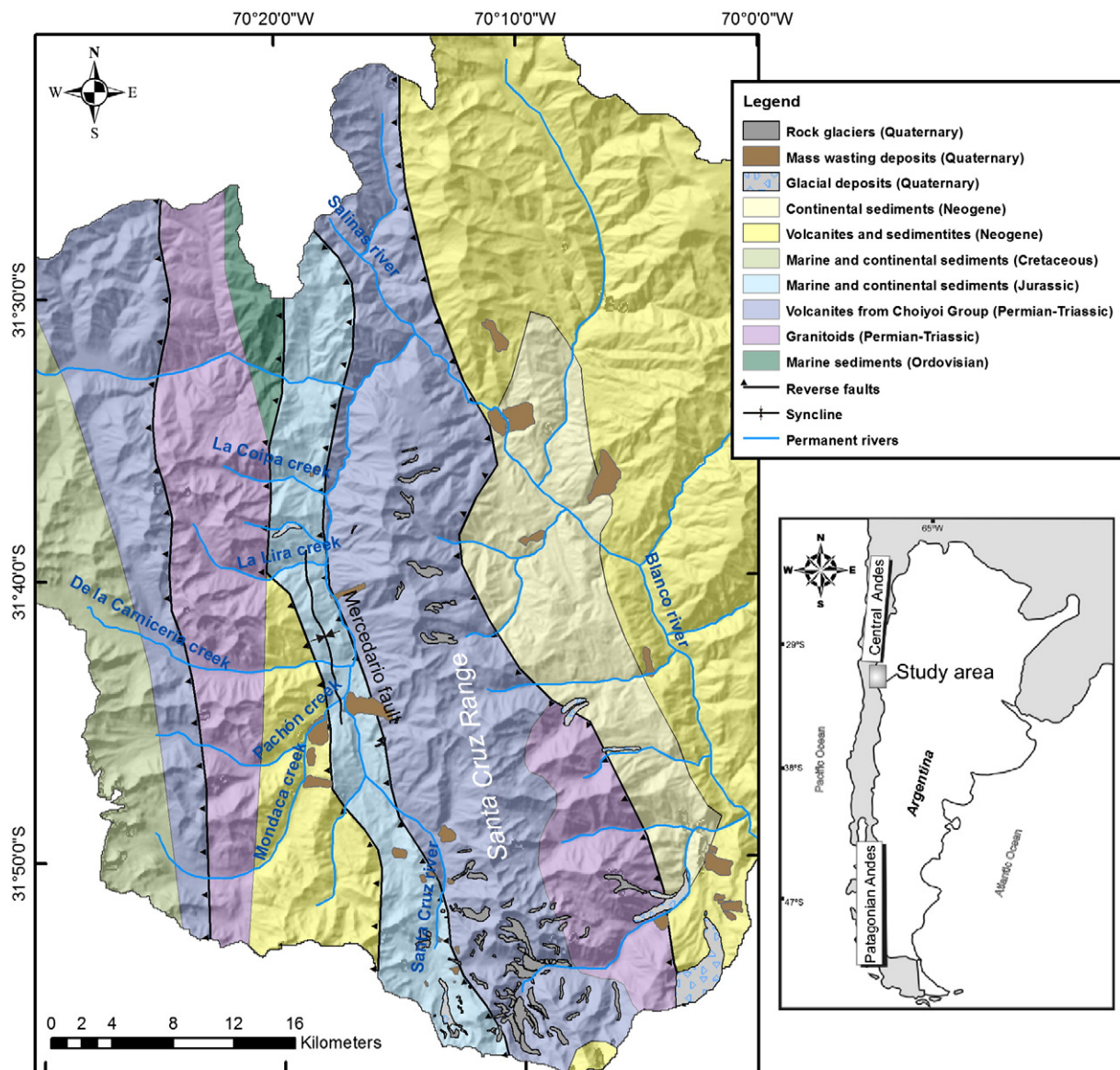


Fig. 1. Geologic-shaded relief map of the study area and main fluvial courses. (Modified from SEGEMAR, 1997).

The Santa Cruz range mean altitude is 3,600 m asl; however peaks such as the Cerro Mercedario (6,770 m asl) stand out in the landscape. Pleistocene glaciation have left a strong imprint on the landscape, as most of the valleys present typical U-shaped cross sections. At the confluence between the De la Carnicería Creek and Santa Cruz River, part of a moraine deposit remains, and near the mouth of De los Bizcochos creek a lateral moraine is very well preserved (Figs. 1 and 2). After glaciers retreated from the valleys, fluvial and periglacial conditions took place. The temporal progress of the glacial retreat is not well

constrained in the area, but in the Mendoza valley (130 km south) glacial retreat is constrained to ~20–15 ka (Espizua, 1993). Glaciogenic and cryogenic rock glaciers are observed at altitudes above 3500 m asl, and blocks detached from slopes because of frost weathering cover the slopes. The tectonic uplift and the surface processes that shaped the landscape have caused the exposure of Permo-Triassic to Jurassic rocks from the Choiyoi Group (volcanites), synrift sediments from the Rancho de Lata Formation (conglomerates and sandstones), marine sediments from the Los Patillos (sandstones) and La Manga

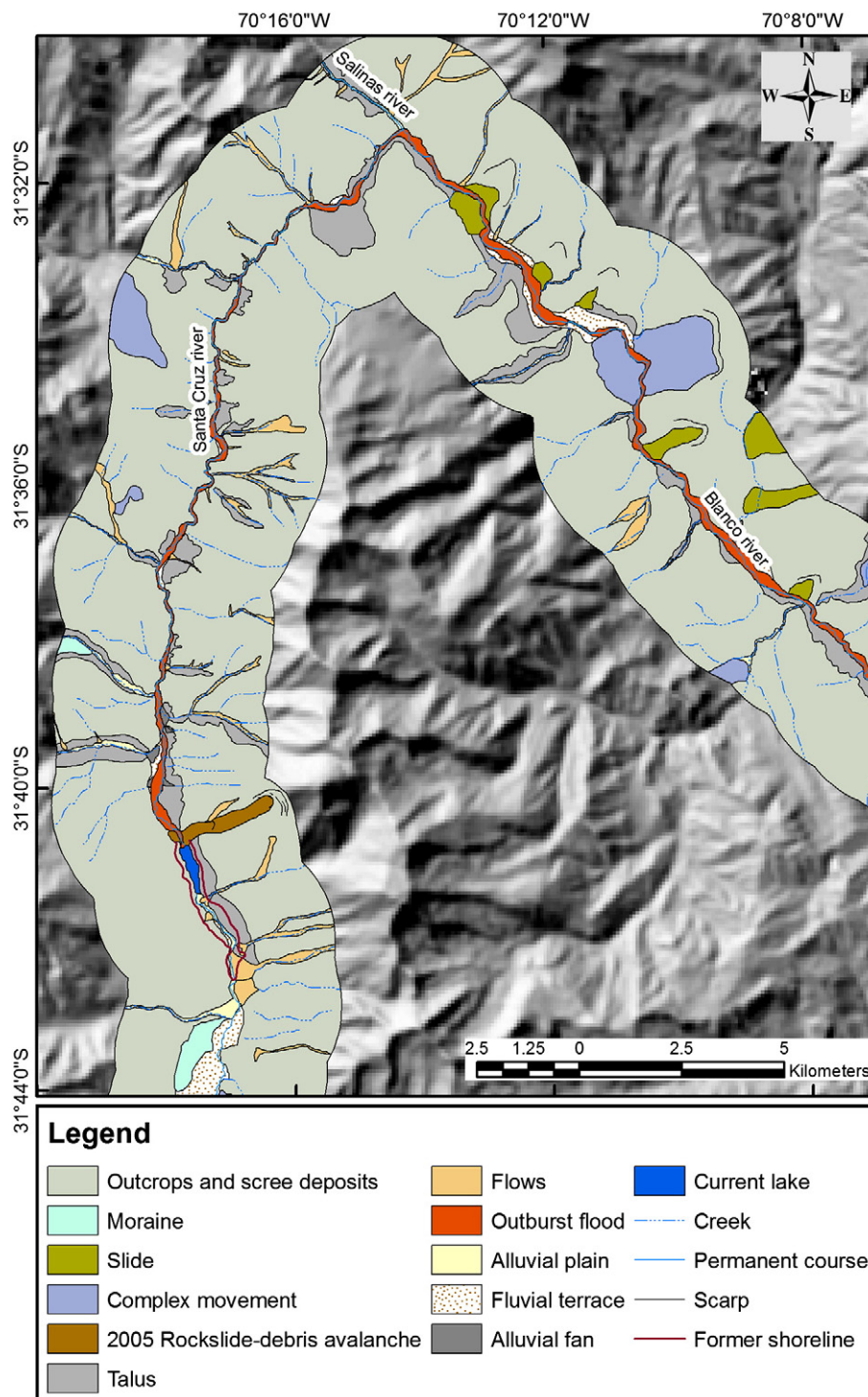


Fig. 2. Geomorphologic map of the study area within a buffer of 2.5 km from the axis of the valley. White areas inside the buffer represents outcrops and minor debris coverage.

(limestones) formations, sag deposits from the Auquilco Formation (evaporites), and continental sediments from the Tordillo Formation (Alvarez and Ramos, 1999).

The climate in the area is dry, with mean temperature in summer (December to March) of around 6 °C, and in winter (June to September) of around −5.7 °C. Extreme temperatures can reach −20 °C, and annual rainfall is around 400 mm, mainly as snowfall during winter (records from Pachón station located at 31°44'S–70°19'S, 3030 m asl; Pereyra, 1996). The hydrographic network is composed by two main courses, the Santa Cruz and Blanco Rivers. The former drains from south to north along 21 km until its confluence with the Salinas River, giving place to the Blanco River that drains NW–SE (Fig. 2). The river discharges are governed by the snowmelt regime, with a pronounced maximum in spring-summer and minimum values during fall-winter (information available at http://www.hidricosargentina.gov.ar/acceso_bd.php; Undersecretariat of Water Resources, Argentina).

3. Materials and methods

3.1. Geomorphologic and structural analyses

The geomorphologic analysis was carried out based on the interpretation of aerial photographs from 1962 (scale 1:50,000), ASTER satellite images, and digital elevation models (DEMs) with pixel size of 15 m from 2003 and 2008 (provided by the National Geologic Survey of Argentina; SEGEMAR), free Google Earth and Landsat Images (available at <http://glcf.umiacs.umd.edu>), field survey, and considering previous studies (D'Odorico et al., 2009; Perucca and Esper Angillieri, 2009). The geologic units and the structural configuration has been derived from the analysis of satellite images and a geologic map from SEGEMAR (1997), except for the Mercedario fault whose location is based on the work of Alvarez and Ramos (1999). Dip direction and angle of the bedding planes in the zone of slope instability were determined using a prototype version of the software ColtopGIS (www.terranum.ch, Crealp), by looking at the continuity of planes on satellite images and a DEM. The volume of rock mass that failed in 2005 was determined through an evaluation of terrain conditions using pre- and post-event ASTER images and DEMs, and the sloping local base level (SLBL) method (Jaboyedoff et al., 2004; Jaboyedoff and Derron, 2005; Jaboyedoff et al., 2009). The SLBL allows us to build a surface above which a certain volume of rock can be detached from a slope. The SLBL requires as input data a DEM, the delimitation of the area collapsed/to collapse, and the curvature of the sliding surface (determined by a slope limit and a factor of tolerance as input parameters). For the 2005 event, we used as input data the 2003 ASTER DEM, a factor of tolerance $C = -0.1$, and slope limits of 12° and 15° in the upper and lower part of the slope, respectively.

An unstable volume of rock bounded by a well developed main scarp has been recognized upslope the headscarp of the 2005 event. Down slope, the limit of these unstable rocks was assumed as the intersection between the base of the Choyoi Group layers and the profile of the slope. In order to evaluate the impacts of future slope failures, we considered two scenarios: a partial failure, comprising rocks bounded by the limit of minor scarps, and a worst case, where all the unstable volume bounded by the major scarp collapses. To assess the threat that can represent potential slope failures, it is important to consider multiple scenarios, as was shown by Hermanns et al. (2011c) in Norway. In both cases, volumes were estimated with the SLBL method using a DEM of 2008, a tolerance factor of −0.1 and a slope limit of 12°.

The inflow rates into the lake were calculated by measuring the changes in volume of the Los Erizos lake, based on the DEM and the sequences of Landsat images documented in D'Odorico et al. (2009). The morphologic changes caused by the outburst flood were assessed by the analysis of ASTER images pre- and post-outburst flood event. The changes in the path of the Santa Cruz and Blanco Rivers from

pre- to post-outburst flood were calculated digitalizing the channel at both stages and measuring their distance difference. The width of the valley floor was computed by digitalizing both margins of the valley. In order to visually assess the modifications occurred to the river bed after the outburst flood, a change detection analysis has been carried out on the two ASTER images. The applied technique consists in performing a pixel-based comparison after nonlinearly matching the statistical distributions of the two images (Volpi et al., 2012a,b). The obtained per-pixel change likelihood has been subsequently spatially segmented in order to obtain a smooth binary change map. Only the differences that occur at the river bed are not filtered out, and the masked change likelihood enhances the different ground cover transitions. This allows a distinction of the river channels before and after the dam failure, as well as the flooded area. We determined the Dimensionless Blockage Index from Ermini and Casagli (2003) for the 2005 dam and the future scenarios based on the volume (V) and thickness (H) of the deposits, and the area (A) of the watershed upstream the dams ($DBI = \log V \times A/H$).

3.2. Dynamic model of landslide propagation

In order to model the dynamic of the slope collapse, we used the DAN3D software (McDougall and Hungr, 2005) that allows, through a back analysis, the simulation of motion of highly mobile landslide using as input data the rupture surface (path-topography), the volume detached (source), and a rheology model chosen by the user (Hungr, 1995; McDougall, 2006; Hungr and McDougall, 2009). To model the 2005 event and the potential scenarios, we used the results of the SLBL as path-topography and source, and chose the Voellmy rheology (frictional-turbulent; Voellmy, 1955), $\tau_{zx} = \sigma_z f + \rho g v^2 / \xi$. τ_{zx} is the basal shear stress, σ_z is total bed normal stress at the base of the mass, f is the friction coefficient, ρ is material density, g is the gravitational acceleration, v is the averaged-depth velocity, and ξ is the turbulence parameter. A turbulence (ξ) of 150 m/s² and a friction coefficient (f) of 0.4 (dimensionless) were the parameters that best fit with the extent and depth of the 2005 event. However, the lack of direct observations, because it took place in a remote place of the Andes, limited the constrain of the input parameters related to the duration and velocities of the landslide. For the potential scenarios, landslide propagation is based on the same rheology model and input parameters as for the 2005 event, and the path topography and source volume were also obtained with the SLBL software.

4. Analysis of past events

In the following sections we will analyze the conditioning factors and dynamics of the 2005 rockslide–debris avalanche, as well as the causes and consequences of the catastrophic outburst flood that affected the 12 November 2005 approximately 250 km of the San Juan River valley in the San Juan province. The information obtained will be used in the final step to assess potential future events.

4.1. The rockslide–debris avalanche of 2005

During the first fortnight of January 2005, a slope failure occurred in the east slope of the Santa Cruz valley, close to the mouth of the de la Carnicería Creek (D'Odorico et al., 2009; Fig. 3A). The detachment of rocks at 4320 m asl produced an amphitheatre-shaped headscarp in a sector of the slope that was already in 1962 bounded by a main scarp (Fig. 3B). The detachment mainly involved volcanic rocks from the Choyoi Group that dips 12°W (strike N–S), toward the axis of the valley. In the west slope, marine outcrops are dipping around 44°W (strike N–S), forming the east flank of a syncline (Fig. 4). Based on the DEM data from 2003 and the reconstruction of the sliding surface, we estimated that around 11.5 × 10⁶ m³ of material was removed from the slope during the event (Fig. 3C). Considering a volumetric change

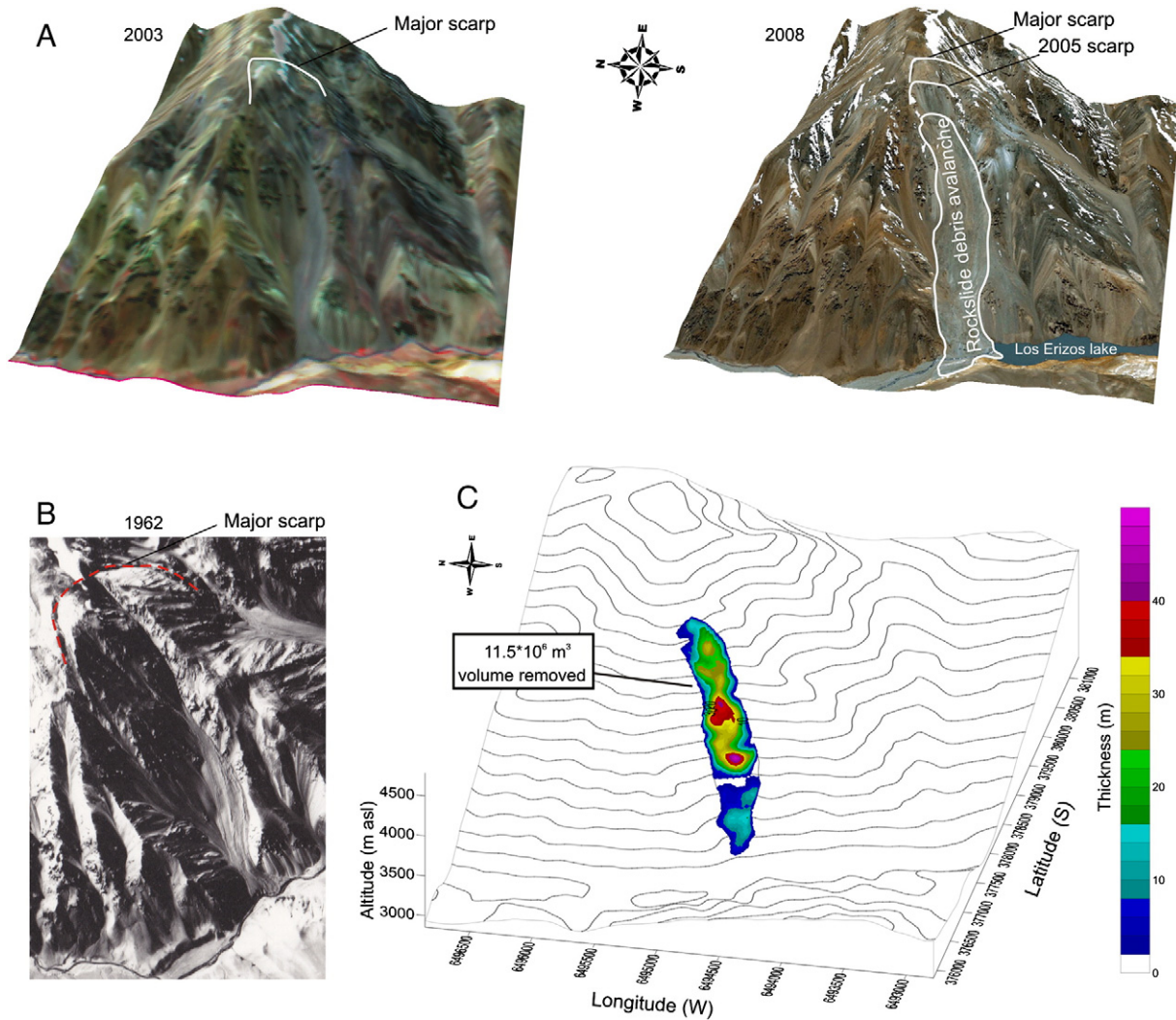


Fig. 3. (A) Three-dimensional views of the eastern slope of the Santa Cruz valley. (B) Aerial photograph from 1962 showing a main scarp well developed (C) Three-dimensional contour map showing thickness and volume of the material removed during the rockslide–debris avalanche from 2005.

of 25% by expansion owing to rock fragmentation (Hungry and Evans, 2004), the volume of the deposit could reach around $\sim 14.3 \times 10^6 \text{ m}^3$. This volume is in the same order of magnitude as the one obtained by Perucca and Esper Angillieri (2009; $12 \times 10^6 \text{ m}^3$), using morphometric

parameters of the deposit. The thickness of the rock detached was greater in the middle part of the slope where a spur of volcanic outcrop was removed, as can be observed comparing pre- and post-failure images. The rock mass displaced down to the valley bottom and ran up

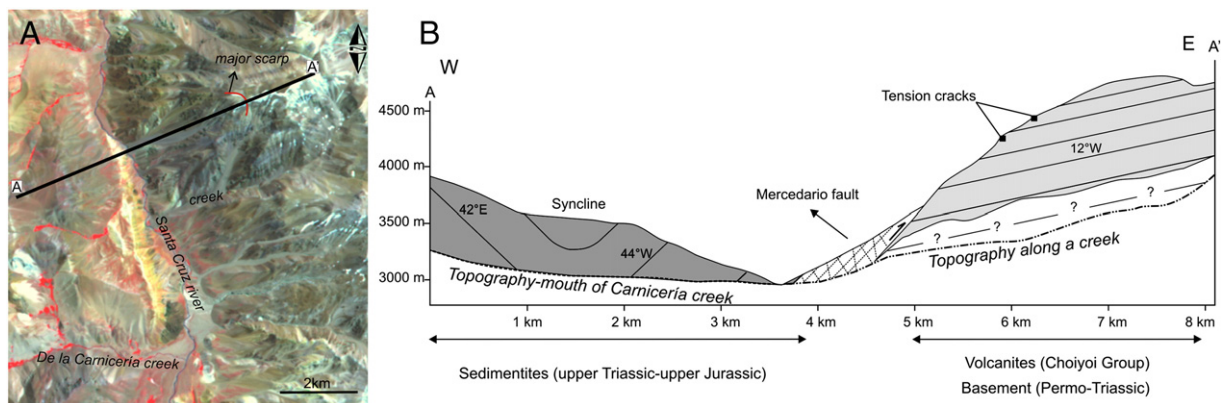


Fig. 4. (A) A 2003 Aster image with location of the cross section for (B). (B) Structural arrangement of outcrops in the segment of the valley where the rockslide–debris avalanche occurred in 2005. The approximate location of the Mercedario fault is based on the map of Alvarez and Ramos (1999), dashed lines represent the deformation zone of the fault. The lower eastern part of the cross section is covered by scree deposits.

the opposite flank of the valley (up to 2980 m asl). This produced the blockage of the Santa Cruz River, and generated the Los Erizos lake, with a contributing watershed area of ~612 km².

4.2. Dynamic model of the rockslide–debris avalanche

The model carried out with DAN3D required as input data the path topography along the materials displaced and the depth of the sliding surface. The path topography resulted from the subtraction of the ASTER DEM of 2003 and the sliding surface determined with the SLBL method. The results obtained using the Voellmy rheology ($\xi = 150 \text{ m/s}^2$; $f = 0.4$) replicates satisfactorily the runout and spreading of the rock mass observed in post-event satellite images (Fig. 5A). When the modeled rock mass reached the valley bottom and impacted perpendicular against the west wall (65 s in the model), the rock mass propagated downstream and upstream, and formed a T-shaped deposit in plain view (Fig. 5A). Its maximum thickness (in the axial part of the valley) was estimated to be around 80 m (Fig. 5A and B), similar to the 71 m obtained by D'Odorico et al. (2009) by field measurements. The maximum thickness is similar to the altitude reached by the Los Erizos lake previous to the dam failure. However, in the distal part (the west slope of the Santa Cruz valley), the estimated thickness of the deposit is lower than the real one. The results of the model show also a good match with the real extent of the deposit, as observed on Landsat images from 24 January 2005. On more recent images, we observed that downstream of the axis of displacement part

of the deposit was eroded during the breaching of the landslide dam. Velocities between 25 and 13 m/s (maximum of 30 m/s) were obtained with the model for the beginning of the movement (Fig. 5C). Then the velocity of the rock mass started to decrease, and at 625 seconds the material reached the state of rest (Fig. 5C). Considering the morphometry of the modeled deposit and the contributing watershed upstream the dam, a blockage index (Ermini and Casagli, 2003) of 3.6 (unstable) was calculated for this dam.

4.3. Causes and effects of the 2005 dam failure

The rockslide–debris avalanche dammed the Santa Cruz River, developing the Los Erizos lake in a sector where the valley floor is around 250 m wide. The lake grew for 11 months until the dam collapsed. Based on the sequence of images from D'Odorico et al. (2009) we estimated minimum inflow rates into the lake, since there is no information about seepage (if there was) through the dam. The inflow between January and February was around 276,000 m³/d, driven by high discharge because of the precipitation season. Minimum inflow rates of 47,000–74,000 m³/d took place between April and October (winter). The maximum inflow rates occurred between late October and the first fortnight of November owing to snow melting and precipitation, with values around 304,000 m³/d. Landsat images of 31 October 2005, show an almost continuous snow coverage in the Santa Cruz range, but in the first fortnight of November the coverage decreased considerably, only being

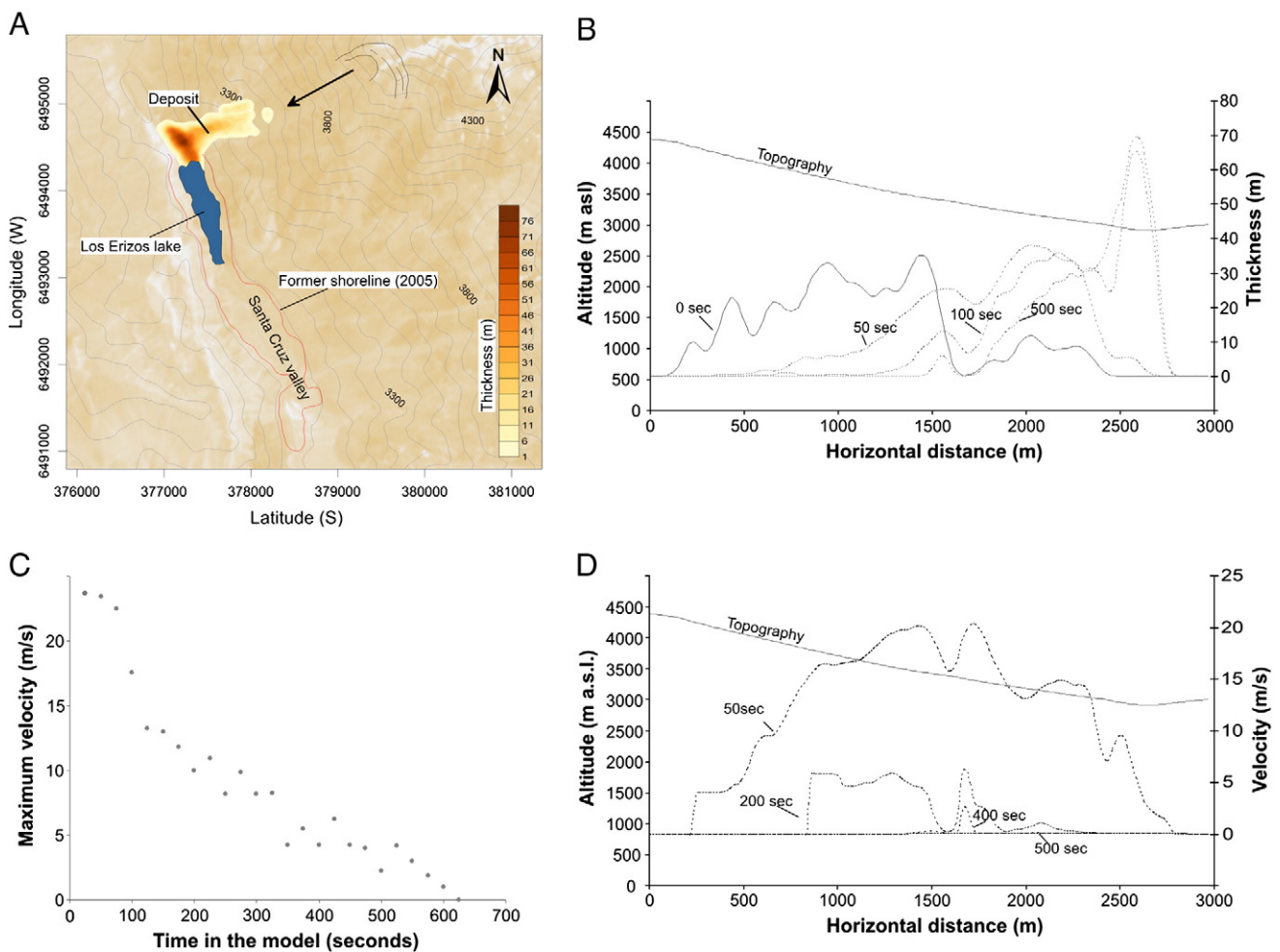


Fig. 5. Back analysis of the 2005 rockslide–debris avalanche propagation. (A) Thickness of the deposit computed with the software DAN3D. (B) Variation of thickness (m) along the topographic profile for different time steps in the dynamic model. (C) Maximum velocity (m/s) of the movement for time steps of 25 s. (D) Variation of velocities (m/s) along the path profile for different time steps of the dynamic model.

present above 3200 m asl. This rapid snowmelt produced the rise in the water level of the lake and could have caused the overtopping on 12 November 2005. The continuity of the pre-dam collapse shoreline located at an altitude of ~2972 m asl, allowed us to determine that the maximum length of the lake was 3.5 km (almost up the mouth of De la Carnicería Creek; Fig. 2), and a maximum volume of water contained in the reservoir of around $30 \times 10^6 \text{ m}^3$. Because of the failure of the natural dam, a trapezoidal breach formed, $24.6 \times 10^6 \text{ m}^3$ of water propagated down the valley, and the sudden decrease of the water level in the lake led to the development of retrogressive slides in the clay deposits from the west slope of the valley (Fig. 6).

The outburst flood modified considerably the geomorphology of the Santa Cruz and Blanco valleys. The mouths of La Lira, De los Bizcochos, and Coipa Creeks (Fig. 1) were forced to change their path toward the north, appearing as *derived* creeks (Fig. 7). The outburst flood entrained sediments from the distal parts of talus, alluvial fans, and terraces and formed small lakes caused by the obstruction of minor creeks. Between the dam and the El Molle mining post, around 10 km^2 of the valley were flooded. Main morphologic changes occurred in sectors where the valley floor is wider, and almost no erosion was recorded in constricted sectors carved into bedrock or large mass wasting deposits (30–150 m valley floor width; Fig. 7A). The paths of the Santa Cruz and Blanco Rivers were modified by the outburst flood. Channel migration up to 198 m was recorded in the Blanco River near its headwaters and immediately upstream of the deposit of a large slope collapse that

generated a gorge in the valley (Figs. 2 and 7B). The outburst flood destroyed the road in several sectors that used to run along the Blanco and Santa Cruz valleys, which provided access to most of the mining projects of the area. In the El Molle post (built over a terrace from the Blanco River) people had to self-evacuate; the infrastructure was seriously damaged and finally abandoned (Fig. 6C). During this event, the gauge station placed in the Blanco River was completely destroyed; people from Barreal and Calingasta localities were evacuated; and in the San Juan River, some facilities of the Caracoles hydropower dam (at that time in the process of construction) were damaged, delaying its inauguration one year. Further details of the outburst flood consequences can be consulted in D'Odorico et al. (2009).

5. Current slope instability – forward analyses of potential runouts

Upslope of the headscarp from the 2005 event, open tension cracks and minor scarps were recognized. These cracks are bounded by a major scarp with a length of 1.5 km, which forms a continuous step of about 15 m high (Fig. 8A). While the main scarp was already seen in aerial photographs from 1962 (Fig. 3B), the tension cracks appeared at an unknown date, but after 1962. Looking at the opening of the tension cracks on a Spot Image from 2008, we measured a total displacement of 12 m, meaning a minimum displacement rate of ~0.25 m/y. Using the limit of minor scarps and the major scarp in the unstable area and the SLBL method, we built two three-dimensional sliding surfaces

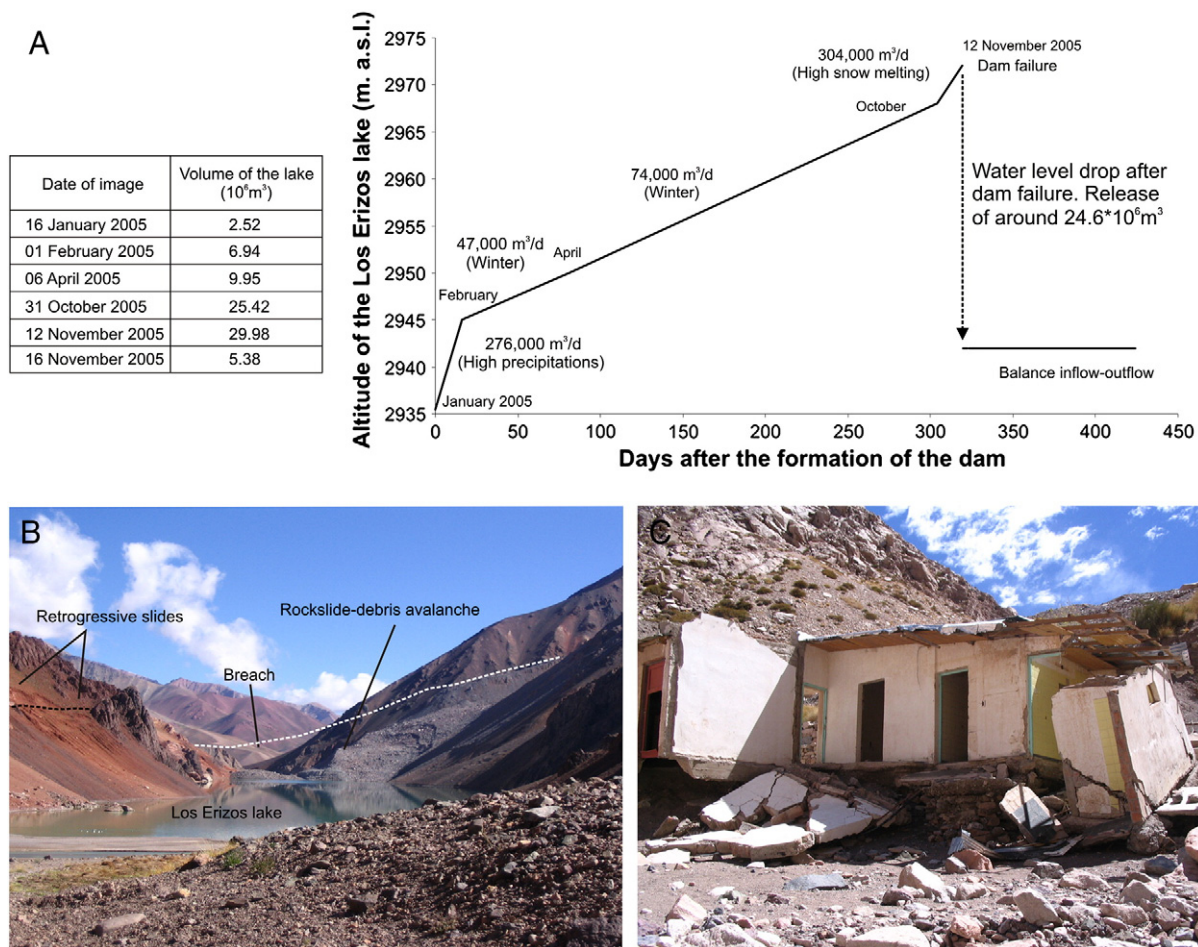


Fig. 6. (A) Hydrograph of the Los Erizos lake water reconstructed from the sequences of images from D'Odorico et al. (2009). (B) View toward the natural dam of the Los Erizos lake, showing the rockslide-debris avalanche deposits, the breach carved during the failure of the dam, and a horseshoe-shaped slope related to retrogressive slides in clay deposits generated after the dam failure. (C) Damages in the El Molle post caused by the outburst flood (75 km downstream the source area).

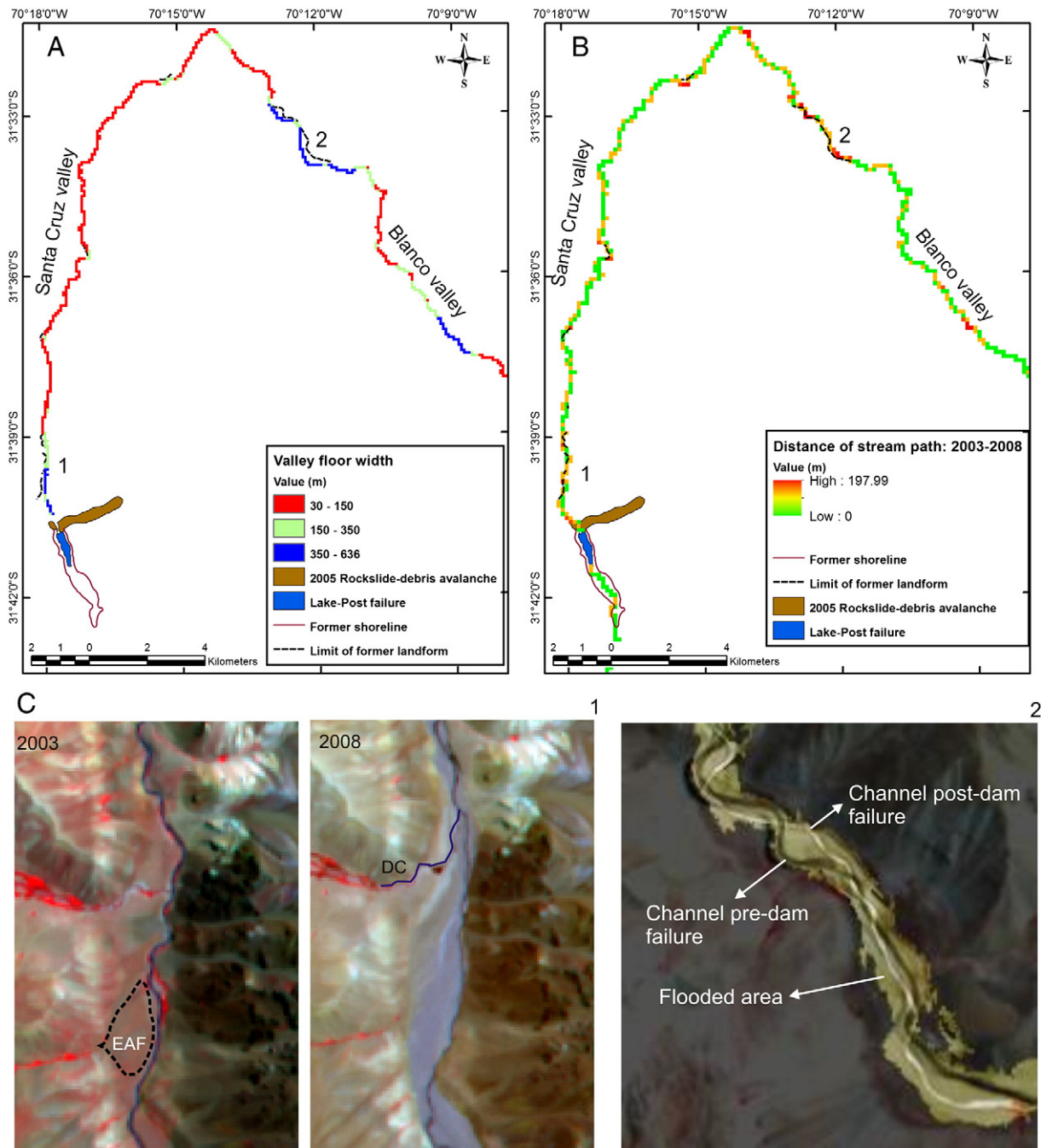


Fig. 7. (A) Variation in the width of the valley floor downstream from the natural dam, and zones where the landforms were eroded. 1 and 2 show locations of pictures in panel (C). (B) Distance between the stream paths prior (2003) and post-outburst flood (2008) of the Santa Cruz River. (C) Satellite images showing some of the morphologic variations recorded in the Santa Cruz and Blanco valleys: (1) erosion of alluvial fan (EAF) and derived creek (DC), (2) changes in the trunk stream and extension of flooded area based on change detection technique.

belonging to a partial slope failure and a worst case scenario (Fig. 8B) and estimated the volumes that could collapse in $6.5 \times 10^6 \text{ m}^3$ and $24 \times 10^6 \text{ m}^3$ respectively (Fig. 8C).

The software DAN3D, used with the rheology and parameters calibrated in the 2005 event, allowed us to estimate the propagation of the rocks for both scenarios. If the rock mass bounded by the minor scarps collapses, materials would propagate in the same direction as the 2005 event, reach the valley bottom of the Santa Cruz River and form a dam (Fig. 8D). In case of a massive collapse (worst case scenario), the model showed that during the propagation, the rock mass would split into two branches: one channeled along the creek located to the

south of the unstable area, and the other one following the same trajectory as the event of 2005. While the materials of the first branch are deposited along a small valley tributary of the Santa Cruz River, the second branch ($\sim 9 \times 10^6 \text{ m}^3$) reaches the valley bottom damming the Santa Cruz River with a maximum thickness of around 75 m. Materials would cover those from the previous event, blocking the breach carved during the failure of 2005 and could partially fall into the current lake. Considering the dimensions of the potential dams and the catchment area upstream, we determined blockage indexes (Ermini and Casagli, 2003) of 3.8 and 3.7 for the first and second scenario, respectively. Both values fall into the instability domain.

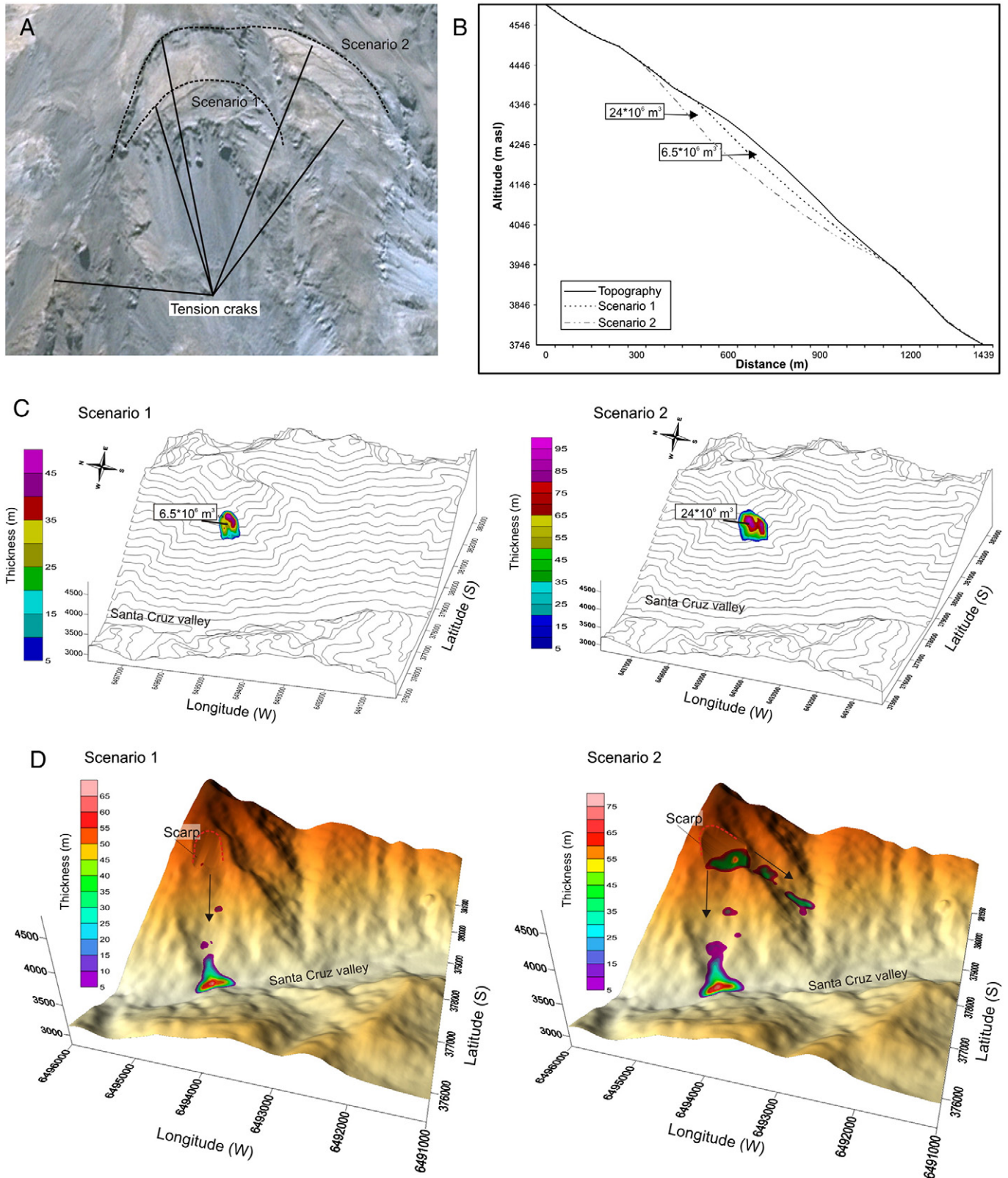


Fig. 8. (A) Spot Image showing the tension cracks present in the slope of the Santa Cruz valley, and the future scenarios considered. (B) Cross section showing the current topographic profile, the potential sliding surfaces and the unstable volumes of rock determined with the SLBL using as input data a factor of tolerance -0.1 and a slope limit of 12° . (C) Three-dimensional contour map showing variations in the thickness and volume for the two scenarios. (D) Spreading of unstable materials for both scenarios modeled with the DAN3D software. Black arrows indicate the direction of propagation of materials.

6. Discussion and conclusions

Abele (1974) noted the strong link between landslide occurrence and faults, showing that in the Alps instabilities are related to major

anisotropies that act as passive conditioning for failures. Also, many works stated the important role of relief in conditioning rockslides, proposing different threshold values that will depend on the rock mass quality (Hermanns and Strecker, 1999; Korup et al., 2007;

Penna et al., 2011). In the Santa Cruz valley, downcutting along the trace of the Mercedario fault exposed in the east wall the deformation zone of the fault and volcanic rocks dipping toward the axis of the valley, providing suitable conditions for the 2005 slope failure. However, the major scarp that bound the area where materials detached in 2005 already existed before 1962. The slope failure did not coincide with the period of heavy snowmelt; and although it occurred during the rainy season, no anomalous rainfall events were recorded at that time. Seismic activity has been continuous in the area and surroundings, where large magnitude earthquakes have taken place such as the $M_s = 7.8$ of 1985 (Beck et al., 1998), without triggering any movements in the slope. This might indicate a process of rock mass degradation driven by progressive slope failure as Eberhardt et al. (2004) proposed for the Randa rockslide in the Swiss Alps. In other words, although none of the individual passive conditioning and potential triggering factors aforementioned were enough to lead to a slope failure, progressive long-term strength degradation might be the causal factor. In such a context, and adding the fact that after the 2005 event the slope gradient increased, the unstable sector of the slope not only did not reach a stable geometry but raised its potentiality for failure, as evident in the open tension cracks. A minimum displacement of around 0.25 m/y measured across these tension cracks suggests a present creep movement preceding a second phase of slope failure.

The dynamic model carried out with DAN3D for the 2005 rockslide–debris avalanche showed how materials propagated upstream and downstream along the axis of the Santa Cruz River forming a landslide dam Type III (Costa and Schuster, 1988) or Type IVa (Hermanns et al., 2011b). The results of the model matches well with the primary morphology of the deposit, later obliterated by the dam failure. If the former extent of a landslide dam is not well established, parameters obtained from the back analysis will be inappropriate to carry out a forward analysis. This will thus impact in the evaluation of hazards related to dam stability, as besides block arrangement and compactation, the geometry and size of the landslide dam have a key role in the dimension of the lake. As shown by Costa and Schuster (1988), landslides whose material form a Type III dam tend to develop larger lakes, implying a higher magnitude of the outburst flood in case of a catastrophic failure. Although, as it is discussed by Manville (2001), the rate of breach growth controlling the peak of discharge will impact on the dynamics and behavior of the flood downstream.

Considering that in the Los Erizos area the Santa Cruz River runs along a narrow section of the valley (even more so since the 2005 dam), and the unstable volume (twice the volume collapsed in 2005), another damming of the valley could occur. This is confirmed by the models carried out with DAN3D, where for both scenarios (a partial slope failure of $6.5 \cdot 10^6 \text{ m}^3$ and a massive failure of $24 \cdot 10^6 \text{ m}^3$) would imply the blockage of the river. From the inventory of dams in the central Andes of Argentina carried out by Hermanns et al. (2011a), the Los Erizos dam was apparently one of the most unstable with a blockage index (Ermini and Casagli, 2003) of 3.6. However, if we considered the study of Costa and Schuster (1988) who showed that 80% of natural dams failures occurred <6 months after dam formation and only 5% lasted between 6 months and 1 year, the Los Erizos dam was actually relatively stable. This indicates that the stability of the Los Erizos dam was dependent on one additional parameter besides the morphometric features of the dam and of the area of watershed upstream from the dam. The fact that the dam formed in January, when the inflow into the lake was low, explains why it took almost one year until its collapse (beginning of November). The dam collapsed when runoff increased considerably because of snowmelt, showing that the climatic context is a key factor determining the life of a natural dam, as was also discussed by Evans et al. (2011) for the Barrancas dam in the southern central Andes. The similar altitude of the paleoshoreline and the top of the dam, and the temporal correlation between the dam failure and a peak in the inflow rate into the lake, indicate that

water level reached a critical value where overtopping was likely to occur. However, as the area is not populated and the lake was not monitored, we can not discard piping or seepage processes aiding the dam breach. From the forward analysis we obtained blockage indexes of 3.8 (first scenario) and 3.7 (second scenario), meaning that dams would also be as unstable as the 2005 dam. As there is currently a lake around 30 m deep, if a rock mass impacts into the water body, the related wave could cause the overtopping of the dam, as occurred in the Las Conchas valley (NW Argentine; Hermanns et al., 2004).

The outburst flood resulting from the 2005 dam failure produced significant changes in the channels and valley floor morphologies of the Santa Cruz and Blanco Rivers. After the outburst flood, the trunk stream migrated in certain sectors around 198 m, higher values than those under normal (climatic-controlled) conditions. The main changes occurred in the wide sections of the valleys, while in narrow sections morphological changes were minimal. Similar patterns of erosion and accumulation were already recognized by Manville et al. (1999) in the Lake Taupo (North Island, New Zealand), by Kershaw et al. (2005) in Queen Bess Lake (British Columbia, Canada), and in Island by Carrivick (2006) among others.

From all the aforementioned and from the presence of vulnerable elements situated in the outburst flood prone area, the analysis of these processes deserve special attention, as well as a need to carry out analysis based on multiple scenarios, as was recently discussed by Hermanns et al. (2011c) with an example in Norway. Monitoring of unstable slopes and all the information that can be obtained during this kind of analysis is critical for land use planning (specially engineering of hydropower dams), hazard mitigation, and emergency management.

Acknowledgments

The authors wish to thank Valerie Baumann and Graciela Marin from the Servicio Geológico Minero Argentino (SEGEMAR), which provided the satellite images, DEMs, and aerial photographs. The authors would like to acknowledge Prof. O. Hungr and Dr. Scott McDougall for valuable comments during the development of this study. We acknowledge the thoughtful reviews from the anonymous reviewers that contributed to improve our manuscript. Dr. Ivanna M. Penna was awarded with a grant from the Swiss Confederation that contributed to this research at the Research Centre for Terrestrial Environment-CRET. M. Volpi was supported by SNSF, project number 200021-126505.

References

- Abele, G., 1974. Bergstürze in den Alpen. Wissenschaftliche Alpenvereinshefte, München: Ausschüsse des Deutschen und österreichischen Alpenvereins, 25, p. 31.
- Alvarez, P.P., Ramos, V.A., 1999. The Mercedario rift system in the principal Cordillera of Argentina and Chile (32° SL). *Journal of South American Earth Sciences* 12, 17–31.
- Baranzagi, M., Isacks, B., 1976. Spatial distribution of earthquakes and subduction of the Nazca Plate beneath South America. *Geology* 4, 686–692.
- Beck, S., Barrientos, S., Kausel, E., Reyes, M., 1998. Source characteristics of historic earthquakes along the central Chile subduction zone. *Journal of South American Earth Sciences* 11 (2), 115–129.
- Carrivick, J.L., 2006. Application of 2D hydrodynamic modelling to high-magnitude outburst floods: an example from Kverkfjöll, Iceland. *Journal of Hydrology* 321, 187–199.
- Clague, J.J., Evans, S.G., 1994. Formation and failure of natural dams in the Canadian Cordillera. *Geological Survey of Canada Bulletin* 464, 1–35.
- Costa, J.E., Schuster, R.L., 1988. The formation and failure of natural dams. *Geological Society of America Bulletin* 100, 1054–1068.
- Cristallini, E.O., 1996. La faja plegada y corrida de La Ramada. *Geología de la región del Aconcagua, provincias de San Juan y Mendoza*. Subsecretaría de Minería de la Nación: Dirección Nacional del Servicio Geológico Argentino, Argentina, 24, pp. 349–386.
- Dai, F.C., Lee, C.F., Deng, J.H., Tham, L.G., 2005. The 1786 earthquake-triggered landslide dam and subsequent dam-break flood on the Dadu River, southwestern China. *Geomorphology* 65, 205–221.
- D'Odorico, P.E., Pérez, D.J., Sequeira, N., Fauque, L., 2009. El represamiento y aluvión del río Santa Cruz, Andes Principales (31°40'S), provincia de San Juan. *Revista de la Asociación Geológica Argentina* 65 (4), 713–724.

- Eberhardt, E., Stead, D., Coggan, J.S., 2004. Numerical analysis of initiation and progressive failure in natural rock slopes—the 1991 Randa rockslide. *International Journal of Rock Mechanics & Mining Sciences* 41, 69–87.
- Ermini, L., Casagli, N., 2003. Prediction of the behavior of landslide dams using a geomorphological dimensionless index. *Earth Surface Processes and Landforms* 28, 31–47.
- Espizua, L.E., 1993. Quaternary glaciations in the Rio Mendoza valley, Argentine Andes. *Quaternary Research* 40 (2), 150–162.
- Evans, S.G., Delaney, K.B., Hermanns, R.L., Strom, A., Scarascia-Mugnozza, G., 2011. The formation and behaviour of natural and artificial rockslide dams; implications for engineering performance and hazard management. In: Evans, S.G., Hermanns, R.L., Strom, A., Scarascia-Mugnozza, G. (Eds.), *Natural and Artificial Rockslide Dams: Lecture Notes in Earth Sciences*, 133, pp. 1–77. http://dx.doi.org/10.1007/978-3-642-04764-0_1.
- González Díaz, E.F., Giaccardi, A.D., Costa, C.H., 2001. La avalancha de rocas del río Barrancas (Cerro Pelón), norte del Neuquén: su relación con la catástrofe del río Colorado (29/12/1914). *Revista de la Asociación Geológica Argentina* 56 (4), 466–480.
- Hermanns, R.L., Strecker, M.R., 1999. Structural and lithological controls on large Quaternary rock avalanches (sturzstroms) in arid northwestern Argentina. *Geological Society of America Bulletin* 111 (6), 934–948.
- Hermanns, R.L., Niedermann, S., Ivy-Ochs, S., Kubik, P.W., 2004. Rock avalanching into a landslide-dammed lake causing multiple dam failure in Las Conchas valley (NW Argentina) — evidence from surface exposure dating and stratigraphic analyses. *Landslide* 1 (2), 113–122.
- Hermanns, R.L., Folguera, A., Penna, I., Fauque, L., Niedermann, S., 2011a. Landslide dams in the central Andes of Argentina (northern Patagonia and the Argentine northwest). In: Evans, S.G., Hermanns, R.L., Strom, A., Scarascia-Mugnozza, G. (Eds.), *Natural and Artificial Rockslide Dams: Lecture Notes in Earth Sciences*, 133, pp. 147–176. http://dx.doi.org/10.1007/978-3-642-04764-0_5.
- Hermanns, R.L., Hewitt, K., Strom, A., Evans, S.G., Dunning, S.A., Scarascia-Mugnozza, G., 2011b. The classification of rockslide dams. In: Evans, S.G., Hermanns, R.L., Strom, A., Scarascia-Mugnozza, G. (Eds.), *Natural and Artificial Rockslide Dams: Lecture Notes in Earth Sciences*, 133, pp. 581–593. http://dx.doi.org/10.1007/978-3-642-04764-0_24.
- Hermanns, R.L., Dahle, H., Bjerke, P.L., Crosta, G.B., Anda, E., Blikra, L.H., Saintot, A., Longva, O., Eiken, T.E., 2011c. Rock slide dams in Møre Romsdal county, Norway: examples for the hazard and potential of rock slide dams. *The Second World Landslide Forum*, Rome, Italy, p. 392.
- Hewitt, K., 1982. Natural dams and outburst floods of the Karakoram Himalaya. In: Glen, J. (Ed.), *Hydrological Aspects of Alpine and High Mountain Areas*. International Association of Hydrology Sciences, 138. IAHS/AISH Publication, Exeter, United Kingdom, pp. 259–269.
- Hewitt, K., 1985. Natural dams and outburst floods: a Pakistan case study. In: Young, G. (Ed.), *Techniques for prediction of runoff from glacierised areas*. International Association of Hydrology Sciences, 149. IAHS/AISH Publication, Wallingford, United Kingdom, pp. 131–135.
- Hewitt, K., 1998. Catastrophic landslides and their effects on the Upper Indus streams, Karakoram Himalaya, northern Pakistan. *Geomorphology* 26, 47–80.
- Hungr, O., 1995. A model for the runout analysis of rapid flow slides, debris flows, and avalanches. *Canadian Geotechnical Journal* 32, 610–623.
- Hungr, O., 2011. Prospects for prediction of landslide dam geometry using empirical and dynamic models. In: Evans, S.G., Hermanns, R.L., Strom, A., Scarascia-Mugnozza, G. (Eds.), *Natural and Artificial Rockslide Dams: Lecture Notes in Earth Sciences*, 133, pp. 463–477. http://dx.doi.org/10.1007/978-3-642-04764-0_18.
- Hungr, O., Evans, S.G., 2004. Entrainment of debris in rock avalanches: an analysis of a long run-out mechanism. *Geological Society of America Bulletin* 116, 1240–1252.
- Hungr, O., McDougall, S., 2009. Two numerical models for landslide dynamics analysis. *Computers and Geosciences* 35 (5), 978–992.
- Jaboyedoff, M., Derron, M.-H., 2005. A new method to estimate the infilling of alluvial sediment of glacial valleys using a sloping local base level. *Geografia Fisica e Dinamica Quaternaria* 28 (1), 37–46.
- Jaboyedoff, M., Baillifard, F., Couture, R., Locat, J., Locat, P., 2004. Toward preliminary hazard assessment using DEM topographic analysis and simple mechanic modeling. In: Lacerda, W.A., Ehrlich, M., Fontoura, A.B., Sayo, A. (Eds.), *Landslides Evaluation and Stabilization*. Balkema, Rotterdam, The Netherlands, pp. 191–197.
- Jaboyedoff, M., Couture, R., Locat, P., 2009. Structural analysis of Turtle Mountain (Alberta) using digital elevation model: toward a progressive failure. *Geomorphology* 113, 5–16.
- Kershaw, J.A., Clague, J.J., Evans, S.G., 2005. Geomorphic and sedimentological signature of a two-phase outburst flood from moraine-dammed Queen Bess Lake, British Columbia. *Earth Surface Processes and Landforms* 30, 1–25.
- Korup, O., 2004. Geomorphometric characteristics of New Zealand landslide dams. *Engineering Geology* 73, 13–35.
- Korup, O., Clague, J., Hermanns, R.L., Hewitt, K., Strom, A.L., Weidinger, J.T., 2007. Giant landslides, topography and erosion. *Earth and Planetary Science Letters* 261 (3–4), 578–589.
- Manville, V., White, J.D.L., Houghton, B.F., Wilson, C.J.N., 1999. Paleohydrology and sedimentology of a post-1.8 ka breakout flood from intracaldera Lake Taupo, North Island, New Zealand. *Geological Society of America Bulletin* 111 (10), 1435–1447.
- Manville, V., 2001. Techniques for evaluating the size of potential dam-break floods from natural dams. *Science Report 2001/28*, pp. 72. Institute of Geological and Nuclear Sciences, Wellington.
- McDougall, S., 2006. A new continuum dynamic model for the analysis of extremely rapid landslide motion across complex 3D terrain. [Ph.D. thesis], Department of Earth and Ocean Sciences, University of British Columbia, Canada, 253 pp.
- McDougall, S., Hungr, O., 2005. Dynamic modelling of entrainment in rapid landslides. *Canadian Geotechnical Journal* 42, 1437–1448.
- Pardo, M., Comte, D., Monfret, T., 2002. Seismotectonic and stress distribution in the central Chile subduction zone. *Journal of South American Earth Sciences* 15, 11–22.
- Penna, I.M., Hermanns, R.L., Niedermann, S., Folguera, A., 2011. Multiple slope failures associated with neotectonic activity in the southern central Andes (37°–37°30'S), Patagonia, Argentina. *Geological Society of America Bulletin* 123 (9–10), 1880–1895.
- Pereyra, B.R., 1996. Clima de la provincia de San Juan. *Catálogo de recursos humanos e información relacionada con la temática ambiental de la región andina argentina*. (<http://www.cricyt.edu.ar/ladyot/catalogo/cdandes/cap00.htm#inhalt>).
- Perucca, L., Esper Angillieri, Y., 2009. Evolution of a debris–rock slide causing a natural dam: the flash flood of Río Santa Cruz, Province of San Juan—November 12, 2005. *Natural Hazards* 50 (2), 305–320.
- Ramos, V.A., Aguirre Urreta, M.B., Lencinas, A., 1993. El Toarciano fosilífero de Pachón y su relación con el Jurásico de Cordillera Principal de San Juan. *Proceedings of 12^o Congreso Geológico Argentino and 2^o Congreso de Exploración de Hidrocarburos*, Buenos Aires, Argentina, pp. 94–104.
- SEGEMAR (Servicio Geológico y Minero Argentino), 1997. *Mapa geológico de la República Argentina. Scale 1: 2,500,000*. Secretaría de Industria Comercio y Minería de Argentina, Buenos Aires.
- Sosio, R., Crosta, G.B., Hungr, O., 2008. Complete dynamic modeling calibration for the Thurwieser rock avalanche (Italian central Alps). *Engineering Geology* 100 (1–2), 11–26.
- Voellmy, A., 1955. Über die Zerstörungskraft von Lawinen. *Schweizerische Bauzeitung* 73, 212–285.
- Volpi, M., Tuia, D., Camps-Valls, G., Kanevski, M., 2012a. Unsupervised change detection with kernels. *IEEE Geosciences and Remote Sensing Letters* 9 (6), 1026–1030.
- Volpi, M., Matasci, G., Tuia, D., Kanevski, M., 2012b. Enhanced change detection using nonlinear feature extraction. *IEEE International Geosciences and Remote Sensing Symposium*, Munich (D), Germany, pp. 6757–6760.